DYNAMIC MODEL OF A TWO-STROKE GLOW ENGINE FROM EXPERIMENTAL DATA

Joaquim Neto Dias, joukend@gmail.com
Gustavo Oliveira Violato, gustavoviolato@gmail.com
Cristiane Aparecida Martins, cmartins@ita.br
Instituto Tecnológico de Aeronáutica - ITA Praça Marechal Eduardo Gomes, 50 - Vila das Acácias CEP 12.228-900 - São José dos Campos - SP - Brasil

Abstract. *In the present work, the main objective was to experimentally obtain the most representative linear dynamic model of a two-stroke piston engine for small Unmanned Aerial Vehicle (UAV) applications with low-cost sensors and a friendly, LabView®-based interface. The engine was mounted on a test bed equipped to measure thrust and rotational speed. The throttle lever was actuated on by a standard hobby servo motor, which controlled the carburetor's valve opening. Input signal and data acquisition were performed in a two-layer approach: low-cost hardware, where a micro-controller unit managed the sensor's reading, servo input and external communications through serial protocol; and LabView for command signal generation, serial port write/read, data processing and other high-level tasks. The motor dynamics, represented by its transfer function, was obtained by minimizing the output error between the experimental responses to various types of input signal and that obtained by the simulation of a fixed topology, fixed order reference model that included the servo and engine models in series.*

Keywords: *dynamic model, experimental, glow engine, two-stroke, parameter estimation, systems identification*

1. INTRODUCTION

The knowledge of the dynamic characteristics of the propulsive system is very important to aircraf's control, in order to avoid undesired oscillations when throttle changes are suddenly applied to the aircraft. In fact, the throttle control is so important that it has been used successfully as the only control available to land a severely damaged aircraft as in Hughes and Dornheim (2003).

Besides that, all modern propulsive systems include a package control, such as a FADEC, to maximize the engine efficiency and to stabilish limits in order to preserve the engine's operational life. In both situations cited above, a model of the dynamic response of the engine is essential.

In the present work, the main objective was to obtain experimentally the best model representative of a 0.61 cubic inches two-stroke piston engine. The engine was mounted on a test bed designed to measure the thrust and rotation per minute signals, acquired using LabView® through a serial port. The throttle lever was actuated by a servo motor, that controls the carburetor's valve opening. The command signal was generated by LabView, processed by a micro-controller into a PWM format and sent to the servo motor.

In order to obtain the engine transfer function, a sinusoidal frequency sweep was performed. For higher frequencies, the servo motor dynamics introduced a considerable influence on the throttle lever angle input. Additionally, collecting the actual servo motor position from an internal potenciometer, it was possible to obtain the dynamic model of the servo motor alone. Finally, the influence of the servo dynamics response was eliminated and a pure engine transfer function model was calculated.

2. THE ENGINE

The engine used was an O.S. MAX .61 FX glowplug two-stroke piston engine widely used in RC airplane models. This model was chosen due to availability, its small dimensions and the low costs involved to run it. This engine has one cylinder with a piston attached to the propeller shaft. It has also a throttle lever that controls the carburetor's valve opening. A glowplug positioned at the top of the cylinder's head causes the engine ignition and is kept continuously glowing by the heat that remains inside the combustion chamber after each ignition. The fuel used during the experiments was a commercial type, containing mainly methanol with 10% Nitromethane. The propeller used was the two-bladed APC 13x4. More detailed information can be found at O.S.Engines (2001).

3. TEST METHODOLOGY

The main objective is to obtain the engine dynamics, relating the deflection in the throttle lever to the rotation. However, the servo motor has a particular dynamics, relating a change in the pulse width to an output angle, which influences greatly the results acquired so far. In the tests conducted, the change in the rotation has been related to the change in the PWM signal. So, if the servo dynamics is well known, its influence can be subtracted from the results.

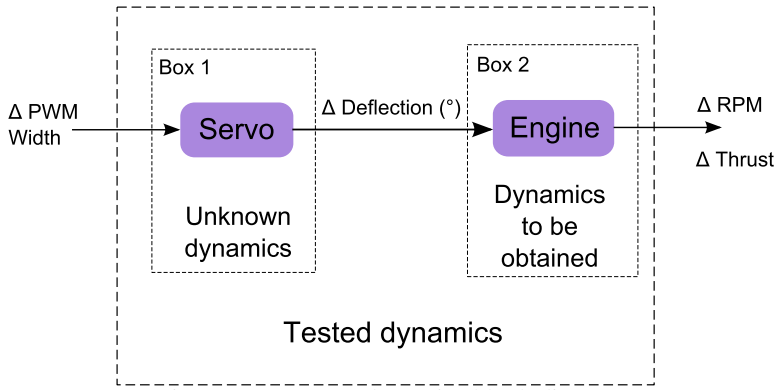

Figure 1: System's dynamics block diagram.

Hence, a test was conducted to obtain the model for the particular servo used in this work. The LabView VI was used to generate a square wave signal. The commanded and actual positions were recorded along time. From these results, a complete servo model was identified. This model was introduced in the Box 1 and, assuming a transfer function model for the Box 2, the results obtained for the whole system (servo + motor) were used to perform the parameter identification for Box 2. The resultant dynamics would be representative of the engine alone and could be used in conjunction with any other servo, as long as the new servo dynamics is known.

4. INSTRUMENTATION

The hardware used in this work consisted of the several modules necessary to perform the tasks of measuring the engine thrust force, the engine RPM, allowing radio communication between hobby transmitter and circuit, idependently commanding the servo actuator and communicating with a standard computer.

The whole achitecture of the istrumentation was based around a low-cost micro-controller unit (MCU). The one chosen for this experiment was the Atmel ATMega168, since it features a programmable serial USART, PWM generation channels, Real Time Counter unit and 10-bit ADC inputs. Also, an open-source compiler and library (avr-gcc, avr-libc) could be used in developing the code, leaving the costs manly to the circuit components, the MCU programmer and the RC hobby equipment (Radio, Receiver and Servo).

The architecture of the system is described by the diagram in figure 2.

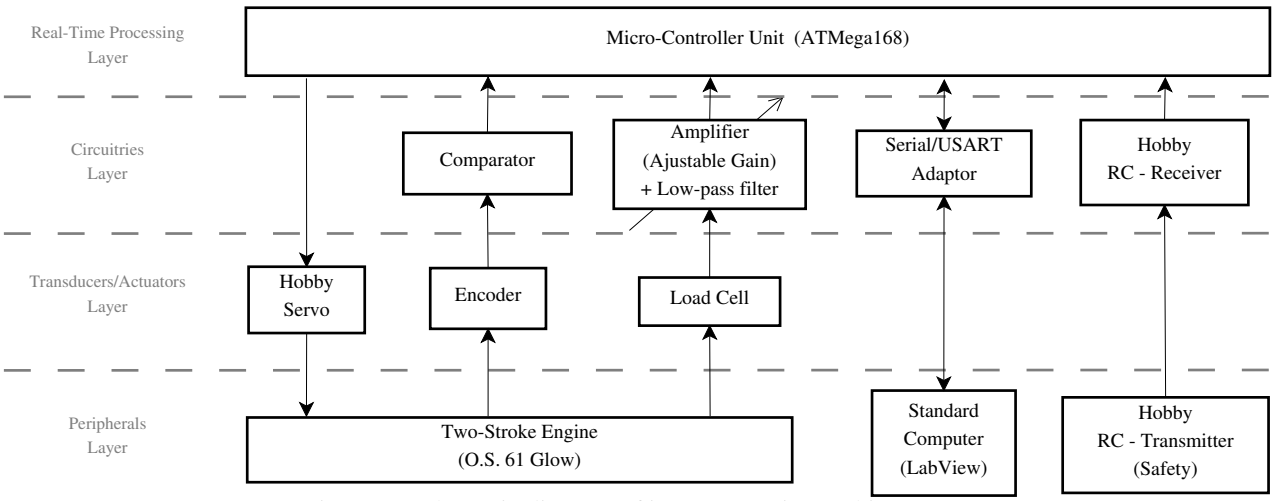

Figure 2: Schematic diagram of instrumentation architecture.

Following is a description of each of the modules connected to the MCU:

Thrust Measurement The thrust was measured by a load cell with four strain gauges in a full-brigde configuration. The brigde was conected to the power suply and to an ajustable gain amplifier system that also filtered the measured signal using a low-pass filter with cut-out frequency of $20Hz$. The output of the filter was fed directly to an ADC input pin in the Micro-controler.

RPM Measurement The rotation was measured using an optical sensor. The sensor consists of an light-emmiting diode and a photo-sensitive transistor and it works by measuring the amount of reflected light comming from itself (figure 3a). A rounded plate with six symmetrical holes was attached to the engine shaft and the optical sensor was mounted behind this plate (3b). The signal coming out of the optical sensor was later modified by means of a comparator circuit, in order to produce suitable square waves to feed the MCU. The sensor worked thus as a regular encoder, with the MCU used to count the time between two consecutive pulses in order to deduce the shafts RPM.

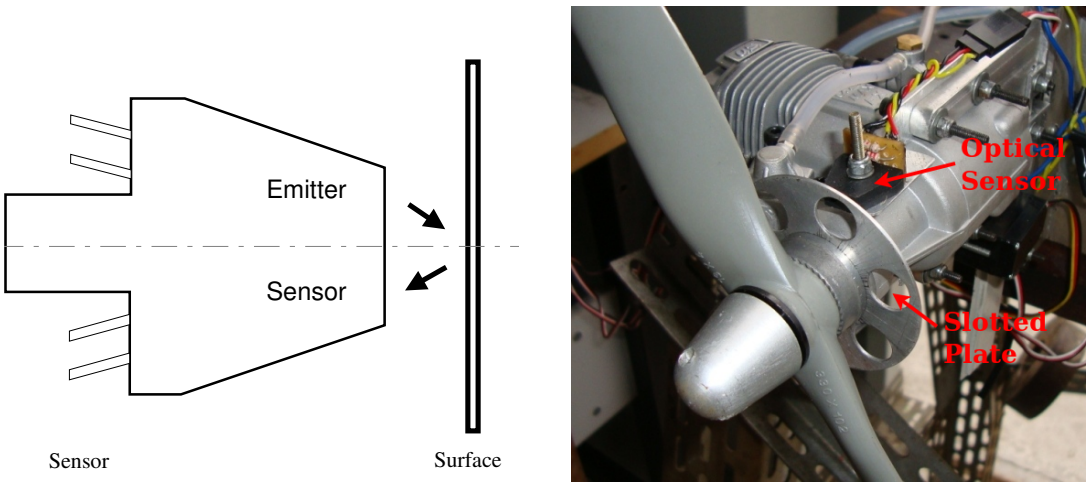

(a) Working principle of the optic sensor. (b) Detail of the RPM measuring set up.

Figure 3: Engine model identification: The step response case.

Throttle lever actuation The throttle lever was actuated on by a standard hobby servo, with a range of 90°. A standard hobby servo command signal consists of a $50Hz$ PWM signal which the duty cycle width varies between $1ms$ and $2ms$. This signal was always fed into the servo by the MCU (figure 2) whether on safe mode, when it was just tunneled from the RC-Receiver to the servo, or on LabView mode, when the desired PWM width came from the serial port. It is important to notice the impact of the $50Hz$ frequency limit of the servo on the dynamics of the combined servo-engine system.

Serial Communication Communication with the computer was accomplished using serial communication protocols (USART\USB). Refer to section 5for more detailed information.

Safety control channel A hobby RC-transmiter radio was used to control the servo position manually during engine startups and eventual needle injection adjustments. The microcontroller was programmed to receive the signal from all six receiver channels. The sixth channel was a toggle switch, which was used to select between "Manual mode" or "Automatic mode". When in manual mode, the servo position was controlled by the radio operator moving the right stick up or down. When in automatic mode, the microcontroller neglected the servo input from the radio and sent the command generated by Labview and received by the serial port. During all tests, at least three signals were acquired at $50Hz$: thrust, RPM and servo motor commanded position.

5. DATA ACQUISITION

The data acquisition was performed using LabView in both cases: manual and automatic control. When in manual control, Labview opens and configures the serial port and then reads continuously the data sent by the microcontroller. The data comes in a string format, which is read until the termination character is recognized, when a new cycle is initiated. At each cycle, Labview splits the string and converts the parameters values to number format. Each new parameter value is plotted in a graph format or shown on LabView's Front Panel. When the loop is stopped, the data is saved into a file and the serial port is closed.

Using manual control, the operator can perform steps inputs in the servo motor. However, the servo response is slower when the signal command comes from the radio. Besides that, the radio controller stick takes an amount of time to travel the whole course, making perfect steps not possible.

To overcome this, the command signals to the servo were generated in LabView. In automatic control, Labview opens and configure the serial port. Two loops are initiated simultaneously and run in parallel. One loop reads data continuously, just like in the manual mode. This loop runs always at $50Hz$, which is the sampling rate sent by the microcontroller. The second loop generates the command signal for the servo. This loop can run at different rates, depending on the type of

command signal desired. However, the maximum rate acceptable is $50Hz$. Since the microcontroller reads always at $50Hz$, any data sent at a rate faster than $50Hz$ will have some points missed by the microcontroller.

6. SIGNAL GENERATION

The VI was designed to allow sending different types of signal and switch between them without aborting the execution. Also, the operator can change the command signal parameters, such as frequency and amplitude.

On a build-up approach, the first signal sent was a constant value, varying manually from minimum to maximum servo range. Using this type of input signal, it was possible to acquire a steady-state value of rotation and thrust parameters from the engine for each servo input value, from idle to maximum thrust.

After that, a square wave signal was developed, between the minimum and maximum values. The square wave frequency could be changed at any time. With this type of input signal, it was possible to collect output signals from rotation and thrust and estimate a transfer function for the whole system (servo + engine), using the LabView System Identification Toolbox.

Another way to obtain the transfer function was applying sinusoidal frequency sweep to the servo motor. Again, on a build up approach, it was first developed a sine wave signal. The engine response was tested since very low frequencies ($0.03125Hz$, i.e. one cycle at each $32s$) until $4Hz$, slighty above the system cutoff frequency. From this test, a Bode diagram could be drawn point by point, where each point would correspond to one frequency tested. However, since no objectionable behavior was observed, a sinusoidal frequency sweep signal was implemented. A new batch of data signals was obtained to be compared with the results obtained from the square wave signal.

7. MAIN RESULTS

7.1 Steady state results

Figure 4 shows the relationships between the PWM signal width sent to the servo and the corresponding thrust and rotation values, from idle to maximum thrust. The errorbar represents a confidence level of 95% ($\pm 2\sigma$).

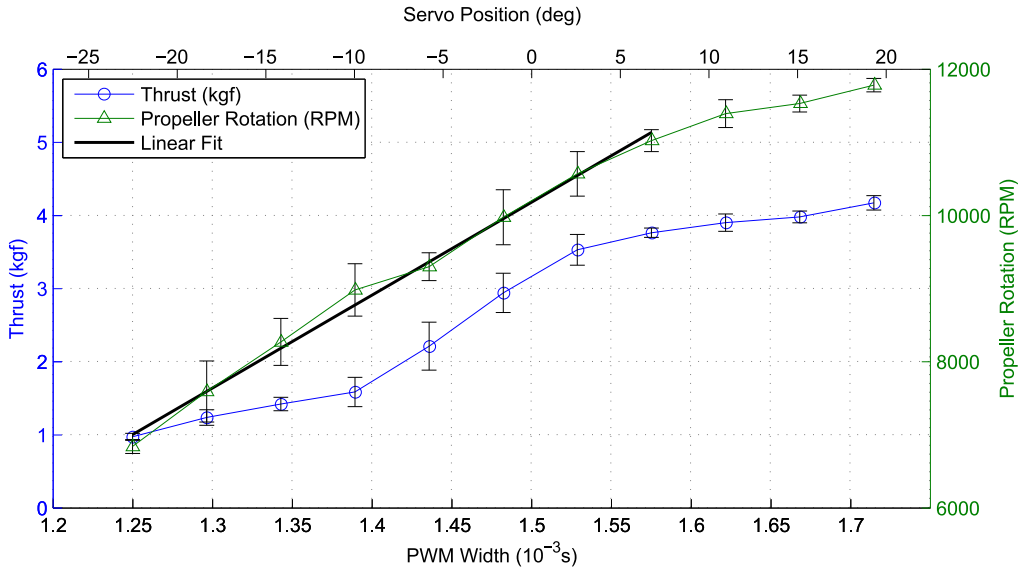

Figure 4: Calibration of steady state values.

The rotation signal response was much more linear than the thrust signal. So, it was defined that the engine transfer function to be obtained would relate throttle lever angle to engine rotation. Above 11000 RPM and below 7000 RPM, some non-linearities were observed. Therefore, the range of servo amplitude for the dynamic tests was defined also: between 7000 and 11000 RPM, for a design point of operation at 9000 RPM.

7.2 Square wave and sinusoidal frequency sweep results

The square wave results are presented in figure 8a. The RPM signal behaves differently depending on the engine is being accelerated or not. Besides that, the dynamic response does not repeat exactly at each cycle: when the RPM is rising, the steady state value for the RPM is achieved on a different way at every cycle. This chaotic behavior introduces more error into the parameter estimation. Hence, becomes interesting to perform a sinusoidal frequency sweep, intending to compare both results.

In figure 9a, the command sinusoidal frequency sweep signal (in terms of PWM signal width) and the response (in terms of variation in RPM) are plotted along time.

Apparently, the response behavior is much more cyclic than the square wave response. Once the servo motor model is known, it will be possible to compare the engine dynamics obtained from the square wave signal and the sinusoidal frequency sweep signal.

7.3 Servo actuator model estimation

In figure 5a, the command square wave signal (in terms of variation of PWM width) and the response (in terms of variation in RPM) are plotted along time.

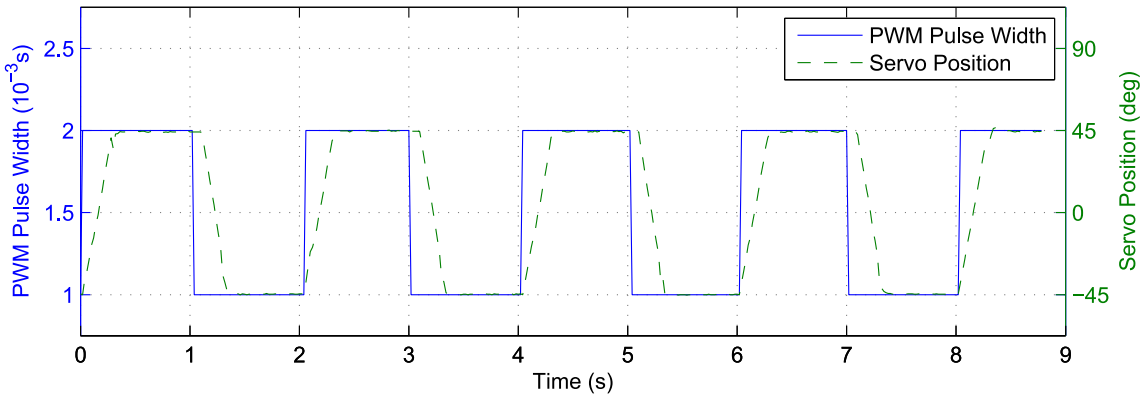

(a) Servo experimental step response.

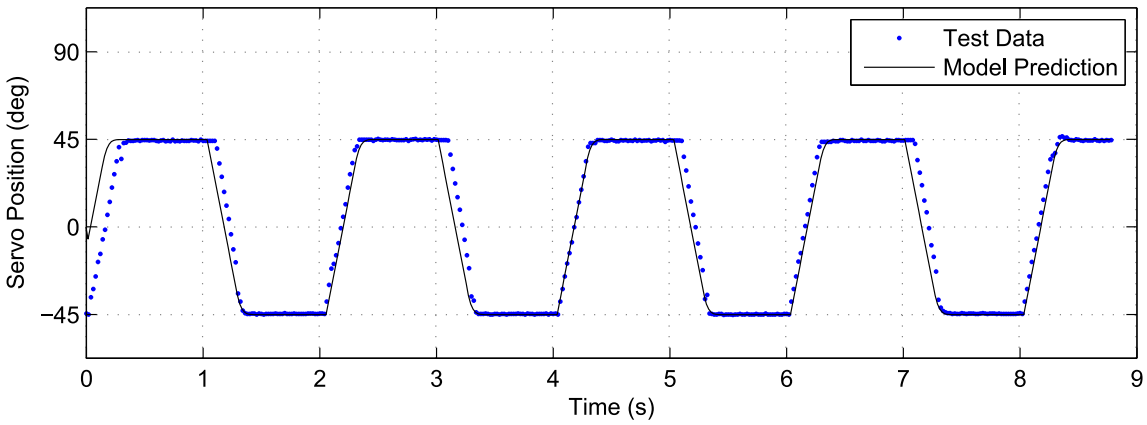

(b) Comparison between indentified model and experimental data.

Figure 5: Servo model identification.

In Brennan (1997) system identification is performed on servos used for RCvehicles. The servos were modeled as a rate-limited second order system. A typical model for a commercial servo motor dynamics is presented in figure 6. Three variables are required to define completely the servo model: gain, pole and saturation.

Using LabView Systems Identification Toolkit, it was possible to create a user-defined model just like the servo model presented in figure 6. The servo model's block diagram created in LabView is shown in figure 7.

With the input and output signals, it was possible to use the LabView's VI SI Estimate User-Defined Model, which employs a Gauss-Newton minimization algorithm to optimize the model variables. The result is presented in figure 6.

Simulating the input signal with the optimized model and comparing the response with the experimental output signal (figure 5b), it can be seen that there is good correspondence bewteen the identified model and experimental data.

7.4 Engine model estimation

Proceeding as explained in section 7.3, after estimating the servo motor model parameters, the engine model was identified. Initially, a first-order model was considered. After estimating the best coefficients, the model was simulated and superimposed with the actual engine response. The first order models estimated with the square wave signal and the sinusoidal frequency sweep signal are presented in the figures 8b and 9b, respectively.

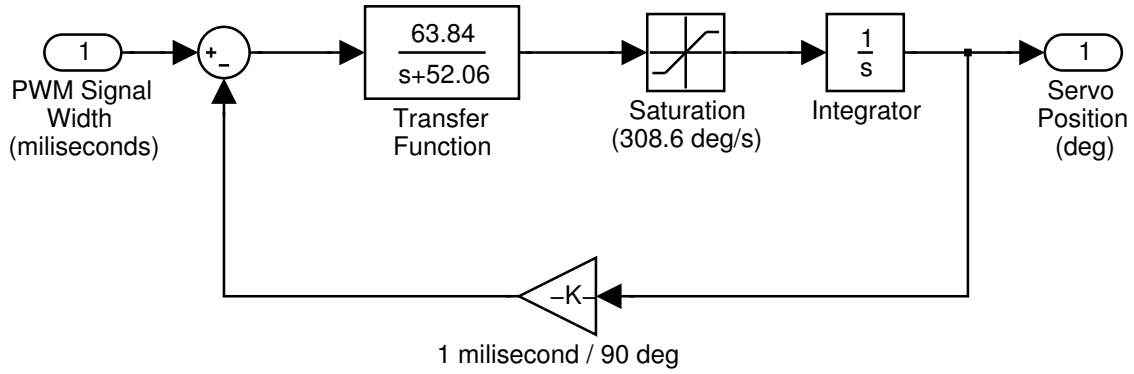

Figure 6: Typical dynamic model for a commercial servo with the identified parameters for this work case.

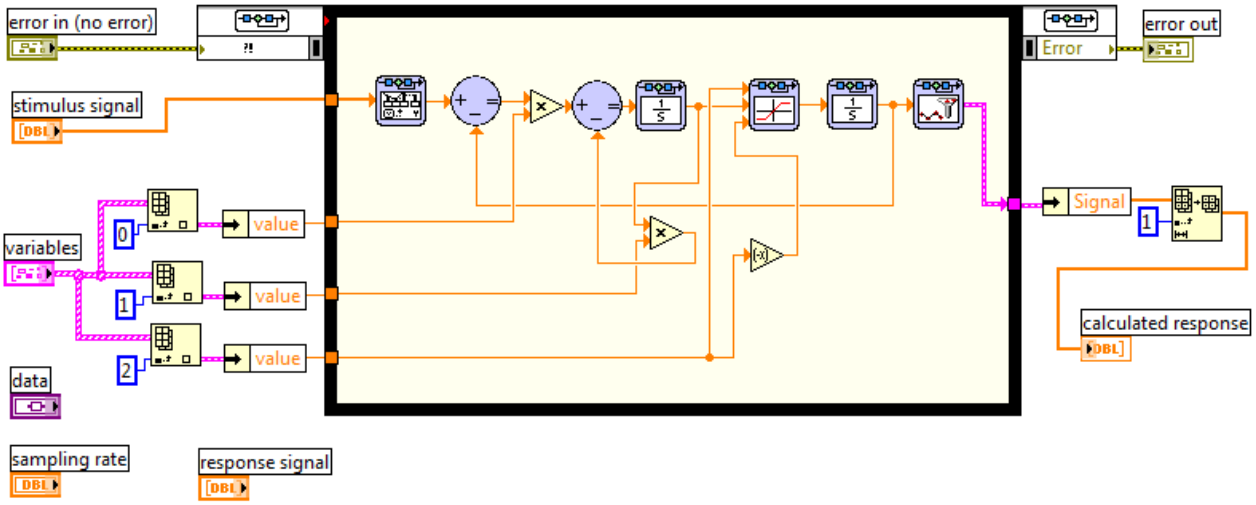

Figure 7: User-defined model for the servo created in LabView environment.

Table 1: Parameter estimation results for sinusoidal frequency sweep and square wave data.

1st-order Transfer Function	Square wave model	Frequency sweep model	Average model
Numerator	549.2	552.7	550
Denominator	s + 4.08	s + 3.90	s + 4.0

Table 1 shows that the estimated parameters from both models are considerably similar. In order to define a 1st-order model to compare with the experimental data in figures 8b and 9b, an average value for the parameters was considered.

7.5 Engine model validation

After estimating the engine model parameters, it is necessary to accomplish another step usually called "model validation". In most cases, it's possible to find more than one model structure that seem to adequately fit experimental data. So, the main challenge is how to decide which model is the best one.

In the previous section, it was presented the 1st-order transfer function obtained for the engine. It was seen that both parameter estimation processes carried out from sinusoidal frequency sweep data and from steps data lead to the same model, but there's no guarantees that this is the best model. Increasing the order of the transfer function usually improves the match between model and experimental data. On the other hand, a more complex model can incorporate errors due to incompatibilities with the actual process being modeled. According to Jategaonkar (2006), if different models can fit the experimental data within specific tolerances, than the best model is that with the minimum number of parameters.

The whole parameter estimation process was repeated for a second-order transfer function model, in order to check if a higher order model would significantly improve the match. This process was performed with the sinusoidal frequency sweep data and square wave data. The input signals were simulated in this 2nd-order model and the output results were compared with those previously obtained by the 1st-order model, as shown in figure 10.

It can be seen that the results are visually coincident. For the sinusoidal frequency sweep data, the differences are

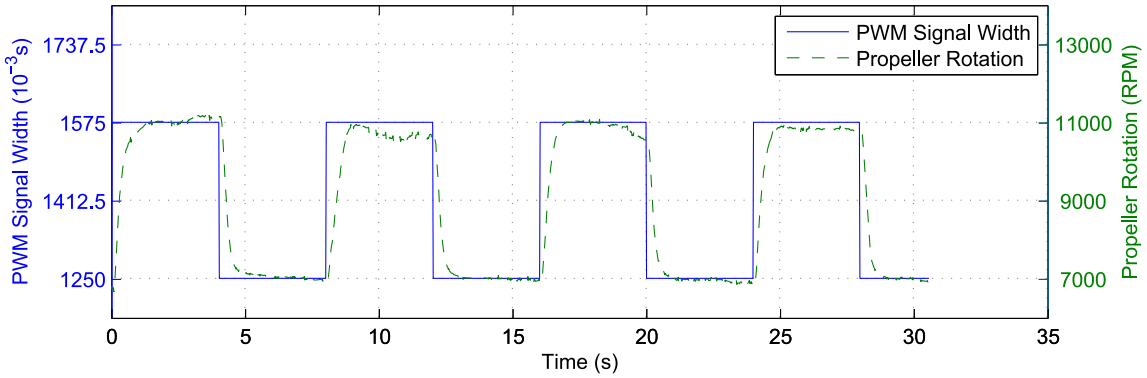

(a) Engine response to square wave signal.

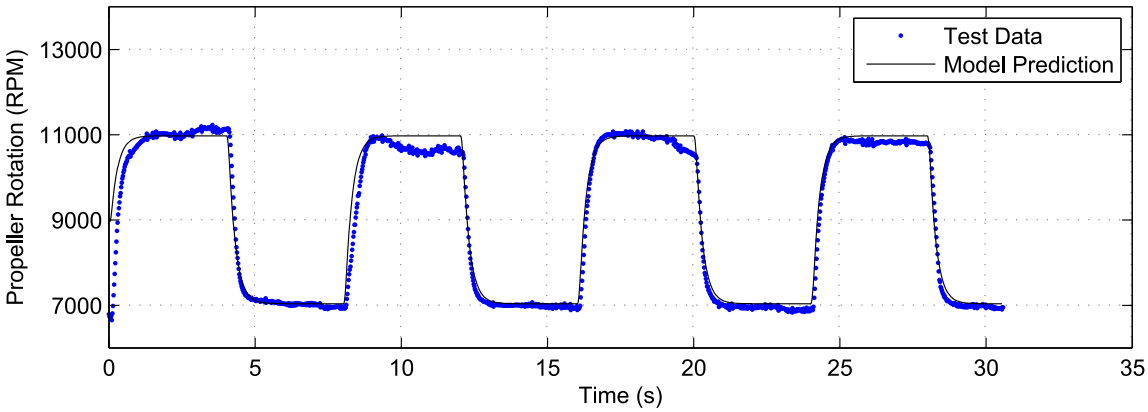

(b) Comparison between indentified model and experimental data: The square wave response

Figure 8: Engine model identification: The step response case.

Table 2: 2nd-order model obtained from parameter estimation.

2nd-order Transfer Function	Model obtained
Numerator	14000
Denominator	$s^2 + 102.7s + 24.3$

less than 4%, while the differences in the square wave data are less than 1%. Therefore, if the match improvement is neglectable, it doesn't seem plausible to develop a more complex model and the first-order transfer function for the engine can be assumed as the best model. The final block diagram with identified parameters is presented in figure 11.

8. CONCLUSIONS

The linear dynamic model of a two-stroke piston engine for small UAV applications was experimentally obtained, with low-cost sensors and a friendly, LabView-based interface. The servo motor used to operate the carburetor's valve introduced a considerable influence on the throttle lever angle input. A user-defined model was developed in LabView and a nonlinear model for the servo motor was identified.

The instrumentation and test methodology were described and it was shown that the model obtained has a good agreement with the experimental data.

We believe that the same test procedures could be applied to more powerful engines, installed in a proper test bed instrumented similarly.

Another objective achieved in this work was to design and use an experimental assembly that can be boarded on a small radio-controlled plane. For a future work, in order to a maintain a desired RPM, a PID controller can be designed and implemented on a micro-controller.

Combined with an indication of true airspeed, this micro-controller could be used aboard a propeller-powered UAV to achieve and maintain a desired thrust level. Besides that, it could be used for in-flight thrust measurements to evaluate the aircraft's overall drag.

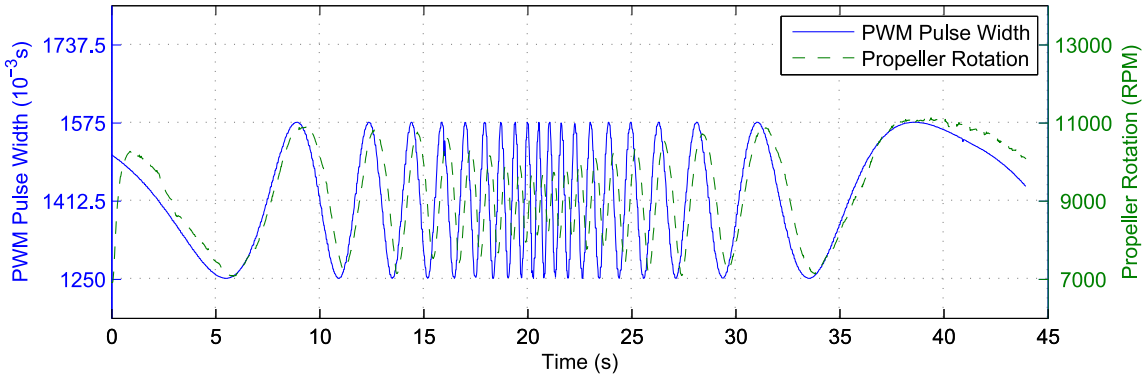

(a) Engine response to sinusoidal frequency sweep signal.

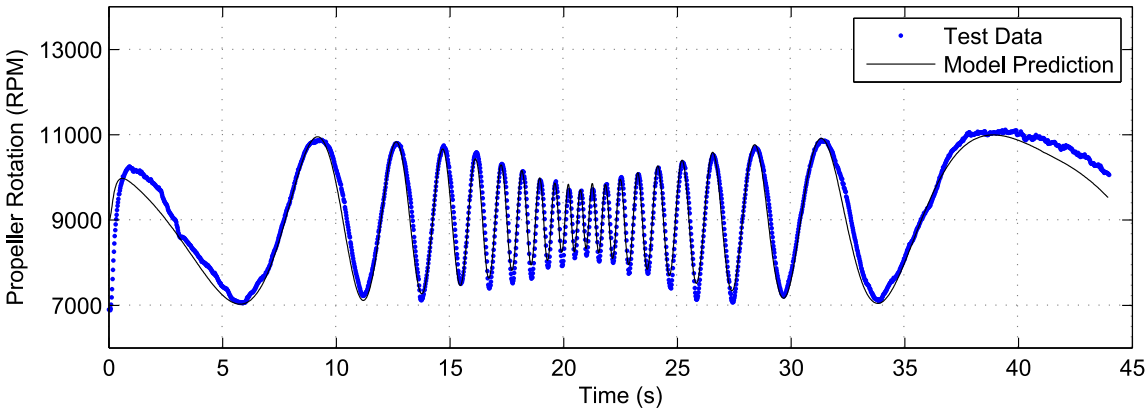

(b) Comparison between indentified model and experimental data: The sweep response

Figure 9: Engine model identification: The sinusoidal sweep case.

The engine model obtained in this work is representative of the transient behaviour of the engine in a particular condition: static thrust. Using a wind tunnel, we believe it would be possible to repeat the same tests to determine the influence of the airspeed in the model.

9. REFERENCES

Brennan, S.N., 1997. *Modeling and Control Issues Associated with Scaled Vehicles*. Master's thesis, New Mexico State University, New Mexico.

Hughes, D. and Dornheim, M.A., 2003. "No flight controls". 8 Dec. 2003, Aviation Week & Space Technology, pp. 42-43.

Jategaonkar, R., 2006. *Flight Vehicle System Identification: A Time Domain Methodology*. AIAA, Reston, Virginia.

O.S.Engines, 2001. *Engine 50SX, 40, 46, 61, 91 'FX Series' Owner's Instruction Manual*. O.S. Engines Mfg. Co., Ltd., Osaka, Japan.

10. Responsibility notice

The authors are the only responsible for the printed material included in this paper.

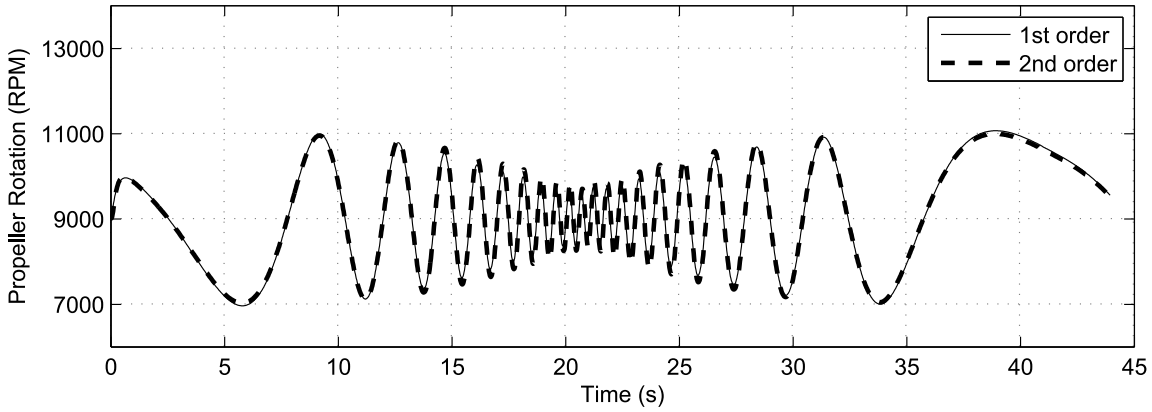

(a) Comparison between 1st-order and 2nd-order estimated models.

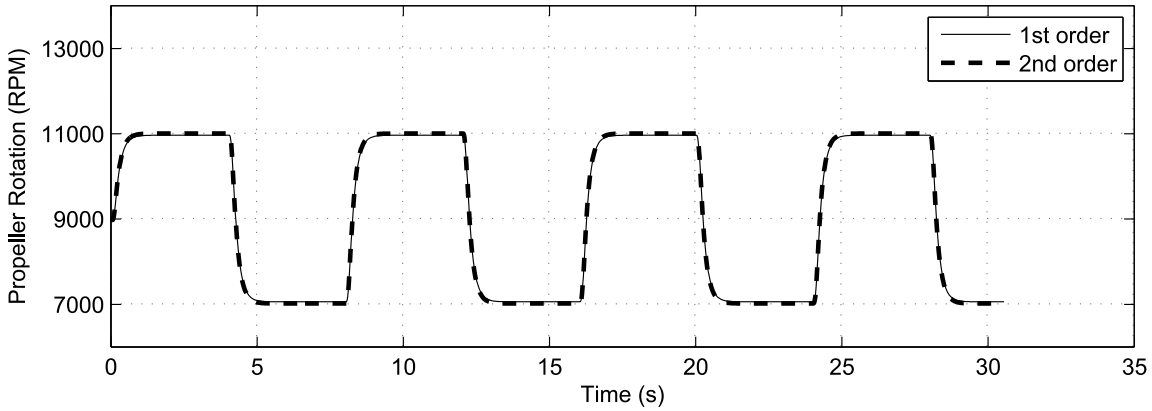

(b) Comparison between 1st-order and 2nd-order estimated models.

Figure 10: Engine model validation: The sinusoidal sweep and square wave case.

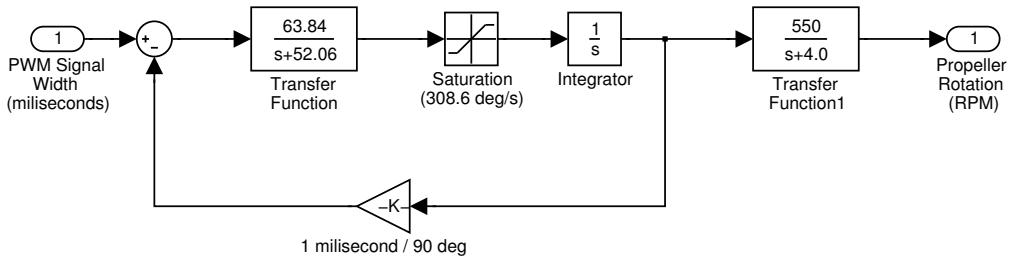

Figure 11: Final block diagram with identified parameters.